Copyright © 2008 Year IEEE. Reprinted from IEEE International Electron Devices Meeting, 15 - 17 Dec 2008, USA. This material is posted here with permission of the IEEE. Such permission of the IEEE does not in any way imply IEEE endorsement of any of Institute of Microelectronics' products or services. Internal or personal use of this material is permitted. However, permission to reprint/republish this material for advertising or promotional purposes or for creating new collective works for resale or redistribution must be obtained from the IEEE by writing to pubs-permission@ieee.org.

The Chemistry of Gate Dielectric Breakdown

X. Li[1,2], C. H. Tung[2], K. L. Pey[1,#], and V. L. Lo[1]

[1]School of EEE, Nanyang Technological University, Nanyang Avenue, Singapore 639798. [#]Tel: 65-67906371, Fax: 65-68989624, email: eklpey@ntu.edu.sg, [2]Institute of Microelectronics, A*STAR (Agency for Science, Technology and Research), 11 Science Park Road, Singapore Science Park II, Singapore 117685.

Abstract

Using scanning transmission electron microscope with high resolution electron energy loss spectroscopy, the chemical nature of the percolation path formed in ultrathin SiON layers is studied for digital and analog breakdown (BD). Our results show that the diameter of the percolation path dilates from 30 nm to 55 nm as the gate leakage current increases from 2 μA to 40 μA. Oxygen deficiency in the percolation path is radially distributed from the BD path center to its surrounding areas. The chemical composition in the center of percolation path changes from $SiO_{1.3}$ to $SiO_{1.0}$ as the BD path evolves from digital to analog BD.

Introduction

The post breakdown (BD) gate leakage current I_g evolution, as shown from multiple-stage constant voltage stress (CVS) [1], is demarcated into two main regions (Fig. 1(a)) by a critical voltage (V_{crit}), where a digitally fluctuated I_g region (Fig. 1(b)) and a stable high leakage region are found.

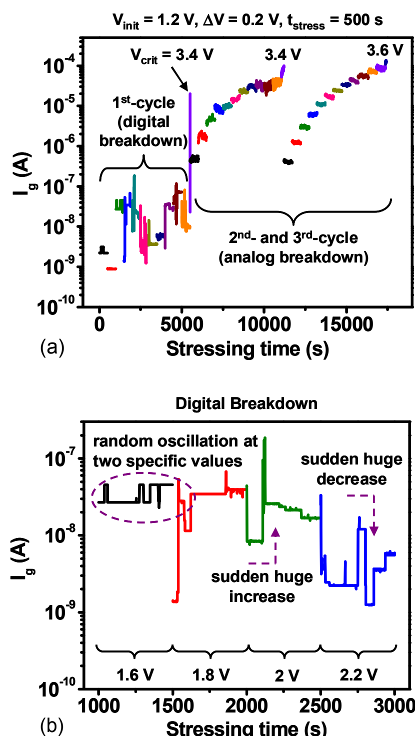

Fig. 1 (a) Post-BD I_g evolution of a BD nMOSFET (22 Å SiO_xN_y and $W \times L$ = 0.6 × 1.0 μm^2) stressed using three-cycle M-CVS. For gate voltage $V_g < V_{crit}$, I_g digitally fluctuates with no apparent net increase. For $V_g > V_{crit}$, I_g rapidly evolves into a stable high leakage state. (b) I_g fluctuation in digital BD region [1].

The oxygen vacancy related defects are believed to be the predominant oxide defect responsible for the pre- and post-BD degradation [2]. E'-centers and neutral oxygen vacancies (V_O) were used to calculate and model the digital fluctuation of post-BD I_g [2]. Despite the theoretical framework, there are limited experimental evidences to show the local chemistry of the percolation path. The understandings of the physical process could provide insightful understanding on the nature of dielectric breakdown.

Experimental Details

For scanning transmission electron microscopy (STEM) and electron energy loss spectroscopy (EELS) analysis, a 2-step CVS was used to create breakdown in the gate dielectric of a metal-oxide-semiconductor transistor in inversion mode at 25°C [1,2]. A high stressing voltage ($V_{gstress}$) of 4.1 - 4.2 V and a low current compliance limit (I_{gl}) of 1 μA were used until a BD occurred. This was followed by a second step stressing with a low $V_{gstress}$ of 3.1 - 3.3 V to achieve the desired breakdown hardness. Since $V_{gstress}$ in Step 2 was larger than the critical voltage V_{crit}, the percolation path could evolve from digital BD to analog BD by controlling I_g [2]. As shown in Fig. 2, two samples - one with I_{gl} of 2 μA (i.e., digital BD) and the other with I_{gl} of 40 μA, corresponding to the region of the digital-to-analog transition, were electrically stressed.

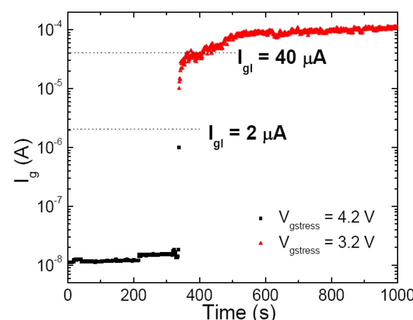

Fig. 2 I_g evolution for a typical 2-step CVS. Two samples with I_{gl} = 2 μA (digital BD) and I_{gl} = 40 μA (analog BD) were prepared for STEM/EELS analysis.

The BD transistors were isolated and thinned down using focused ion beam (FIB) milling to a final thickness of 80 nm (along transistor width direction W as shown in Fig. 3(a)). The samples were cleaned using low energy (2 kV) ion to minimize the damaged layer and *in-situ* lifted-out. The STEM/EELS experiments were performed using a FEI TITAN microscope operated at 80 kV. The STEM probe

1-4244-2377-4/08/$20.00 ©2008 IEEE

size was optimized to be around 3 Å in diameter and the EELS energy resolution was 0.7 eV with 0.05 eV/channel dispersion. Dielectric breakdown induced epitaxy (DBIE) [3] was used as a "nano-marker" to locate the BD spot in the dielectric layer along the transistor channel. A series of line scans, each has 10 probes, of 4 nm apart were conducted at the BD location and its surrounding oxide areas (Fig. 3(b)).

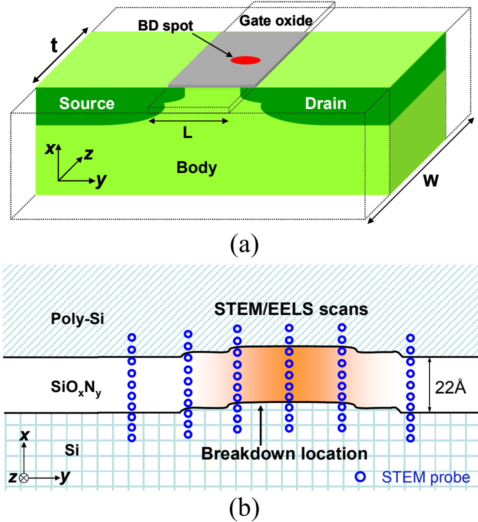

Fig. 3 (a) 3D schematic diagram of the BD transistor after FIB thinning. For presentation purposes, the poly-Si gate and other materials above the dielectric are not shown. The BD spot is included within the TEM sample for EELS analysis. (b) Schematic drawing of the cross-sectional view (x-y plane) of the BD spot in (a), where the EELS line scans shown as dots (3 Å in diameter) from Si substrate/gate oxide/poly-Si were taken at several positions within and in the neighborhood of the BD spot. The spectra at the center of the oxide layer at each line scan are extracted for comparison.

Fig. 4 shows the STEM images of the digital BD sample ($W \times L = 0.15 \times 0.50$ μm^2) where the BD location [4] measured electrically was at 0.36L (L is the effective channel length) from the source terminal and a DBIE bump was found at the corresponding location (Figs. 4(b) & (c)). For the analog BD sample ($W \times L = 0.15 \times 0.20$ μm^2), the BD location was at 0.843L from the source terminal and a defect was found at the corresponding location (Fig. 5(a)). The DBIE defect is only visible in bright field STEM image (Fig. 5(b)) but not so apparent in high angle annular dark field (HAADF) image (Fig. 5(c)). The EELS line scans were performed at the respective BD spot. As illustrated in Fig. 3(b), there are 10 spectra collected across the Si/oxide/poly-Si of the BD and non-BD spot, and those acquired at the center of the gate dielectric of different line scans were analyzed in detail.

Si $L_{2,3}$ edge EELS

Fig. 6 shows the background corrected Si $L_{2,3}$ edge and near edge spectra for the digital BD (Figs. 6(a) & (b)) and analog BD (Figs. 6(c) & (d)) sample at 6 different positions near the BD spot. Positions 1 & 6 are further away from the BD spot while 3 & 4 are at/near the center of the BD spot. Since the Si $L_{2,3}$ edge arises from ionization of Si 2p electrons to the SiO_2 conduction band (CB) unoccupied density of states (DOS), it therefore contains information of Si^{4+} bonding from 105 to 108 eV, and Si^{2+} and Si^{0} bonding onset at 103 eV and 99.8 eV [5]. As discussed previously for ultrathin gate oxide [6], the Si $L_{2,3}$ edge consists mainly of the Si^{4+} signals from the center of the oxide layer and the delocalized signals [7] from the interfacial suboxide [5]. The effective spatial resolution for Si $L_{2,3}$ edge is around 1 nm. Figs. 6(b) & (d) show the spectra at Position 1 to 3 for the two samples, respectively. Both the digital and analog BD sample show a lowered Si^{4+} signal around 108 eV but a raised signal from 100 to 106 eV. The changes in the peak intensities are resulted from the rearrangements of the local CB DOS, which is extremely sensitive to the local atomic bonding structures. In both cases, there is a formation of suboxide SiO_x with $x < 2$ and an edge onset (CB) lowering within the BD spot. The Si^{1+} and Si^{2+} signals were detected for location as labeled in the figures.

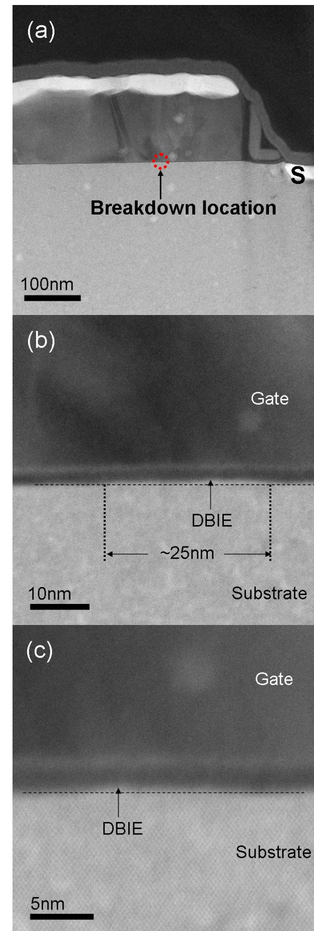

Fig. 4 Cross-sectional STEM HAADF images of a digital BD sample (I_{gl} = 2 μA) (a) Low magnification image where the BD location is marked in the circle at 0.36L from the source terminal. (b) & (c) High resolution (HR) STEM images showing a DBIE bump of 25 nm at the BD location.

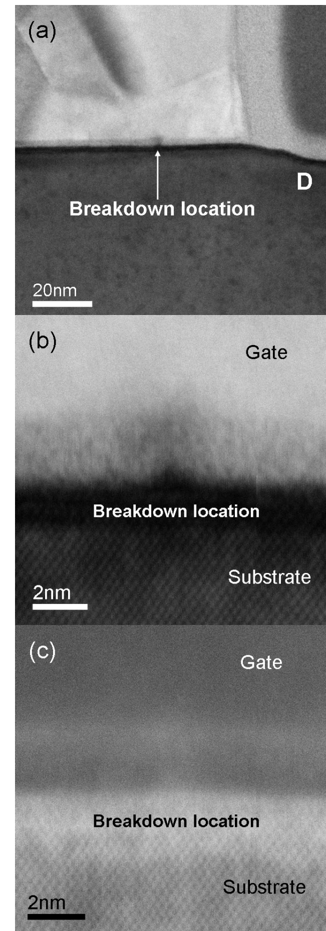

Fig. 5 Cross-sectional images of an analog BD sample (I_{gl} = 40 μA) (a) Low magnification bright field (BF) image where a BD defect was found at 0.843L from the drain terminal. (b) BF HRSTEM image of the defect. (c) The corresponding dark field HRSTEM image acquired simultaneously at the same location.

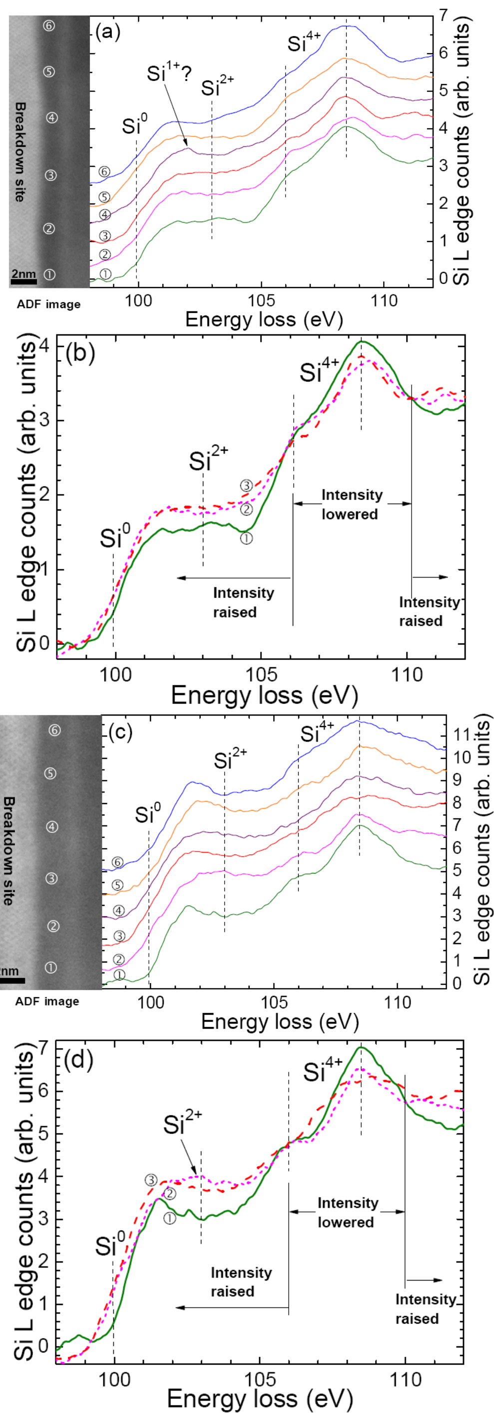

Fig. 6 Background corrected Si $L_{2,3}$ edge EELS collected at the center of the oxide layer for 6 different positions near and at the BD site. Positions 1 & 6 are further away from the BD spot while 3 & 4 are at/near the center of the BD spot. (a) & (b) digital BD; (c) & (d) analog BD. Figures (b) and (d) show the detailed analysis of EELS of Position 1 to 3. The peaks for different Si oxidation states (Si^{0}, Si^{2+} and Si^{4+}) are labeled in the figure. The Si $L_{2,3}$ edge consists of the Si^{4+} signals (105 - 110 eV) from center of the oxide layer with delocalized signals (100 - 105 eV) from the interfacial suboxide. As shown in (b) & (d), the Si^{4+} signals around 108eV of the BD spot are lower but the signals from 100 to 106 eV increased. In both cases, at the BD spot, there is a formation of suboxide SiO_x with $x < 2$ and an edge onset lowering at 100 eV and 105 eV. Si^{1+} and Si^{2+} signals as labeled in the graphs were observed at some positions.

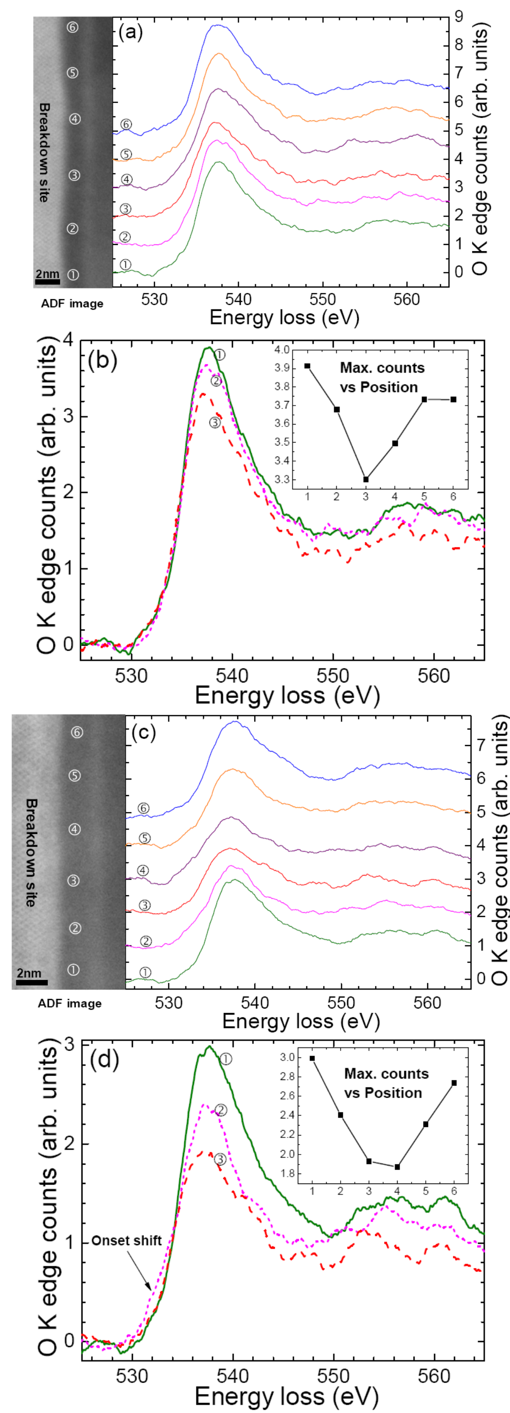

Fig. 7 Background corrected O K edge EELS collected at the center of the oxide layer for 6 positions at and near the BD spot. (a) & (b) digital BD; (c) & (d) analog BD. Figures (b) and (d) show the detailed analysis of EELS of Position 1 to 3. The inserts show the maximum oxygen intensity counts for the 6 positions. The peak at 537.6 eV is originated from the scattering of the ejected O 1*s* electron to its 6 second-nearest neighboring O atoms. As shown in (b) & (d), the drop in the peak intensity when moving to the center of the BD spot implies missing of the neighboring O atoms. There is more O deficiency for the analog BD sample at the BD center. The edge onset lowering is observed at Position 2 in (d). The diameter of percolation path is estimated to be 30 nm and 55 nm for the two BD cases. The intensity counts integrated from 532 to 552 eV are used for the x value calculation in Fig. 9.

O K edge EELS

Fig. 7 shows the background corrected O K edge and near edge spectra for the digital (Figs. 7(a) & (b)) and analog (Figs. 7(c) & (d)) BD sample at 6 different positions. The peak at 537.6 eV is originated from the scattering of the ejected O 1*s* electron to its 6 second-nearest neighboring O atoms (1st O shell) [8] and the peak intensity is related to the amount of O atoms localized at the probing site. The detailed analysis of Position 1 to 3 of the two cases is shown in Figs. 7(b) & (d) where Position 1 is far away from the BD center. The inserts show the maximum intensity oxygen counts for all 6 positions. The diameter of the breakdown path can be estimated using the O K edge spectra by using non-breakdown gate oxide O K edge intensity as a reference.

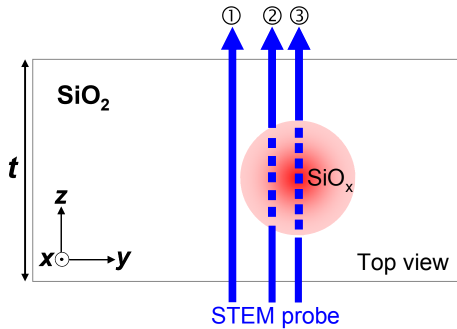

Fig. 8 Schematic diagram showing top view of STEM probe on BD spot (*y*-*z* plane in Fig. 3).

The results show that the estimated diameters of the BD path are 30 nm and 55 nm for the digital and analog BD samples, respectively. The edge intensities from 532 to 552 eV are summed to calculate the deficiency of O. Although the O K edge signals were generated from the entire transmitted sample area (Fig. 8), the drop of the edge intensity is contributed from the percolation path only. Assuming that the defective oxide in the percolation path consists of SiO_x (along *z* direction on average), the O deficiency within the percolation path at every position could be extracted based on the ratio of the transmitted distance in the percolation path (i.e., the dotted lines in Fig. 8) and the sample thickness *t*. Using the non-defective oxide as referenced SiO_2 (e.g., Position 1 with 6 nearest O atoms), Fig. 9 shows the calculated x value (box-plot with 6% variations in the local sample thickness) for the digital (Fig. 9(a)) and analog (Fig. 9(b)) BD samples of all the 6 positions. For the digital BD sample, it is $SiO_{1.3}$ at the BD center probing (Position 3) and $SiO_{1.6\text{-}1.8}$ at the outer shell probing. For the analog BD sample, it is $SiO_{1.1}$-$SiO_{1.4}$-$SiO_{1.7}$ from the most inner to outer shells. The x values imply that there are missing of 1 ($SiO_{1.7}$), 2 ($SiO_{1.3}$) and 3 ($SiO_{1.0}$) O atoms in the 1st O shell (out of 6 if fully occupied) localized at the probing position (illustrated in the inserts in Fig. 9). The smallest x (at the BD center) has values of 1.3 and 1.0 for the digital and analog BD, which is believed to be responsible for the increment in I_g in the analog BD region.

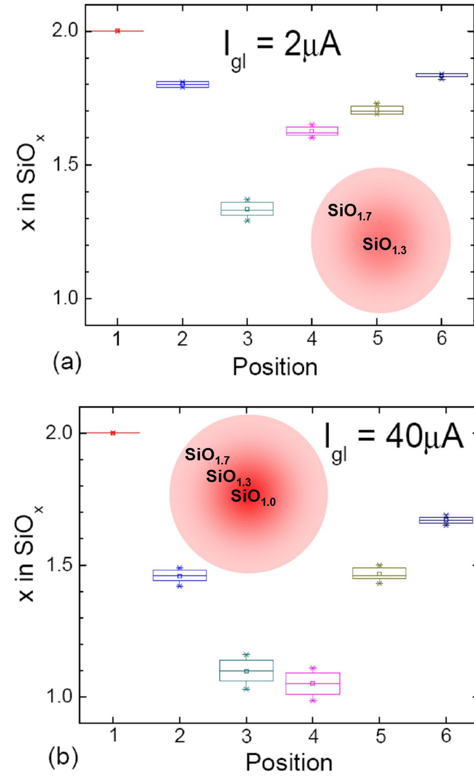

Fig. 9 Calculated x value in the percolation path (SiO_x) for (a) digital & (b) analog BD samples. The inserts show the radial chemical distribution of SiO_x in the digital and analog BD path.

Summary

In conclusion, the EELS results show that the O-deficiency within a percolation path is radially distributed from the BD center to its surrounding areas. The diameters of percolation path dilate from 30 nm to 55 nm when the leakage increased from 2 μA to 40 μA. Based on our finding, for sub-30nm technologies, the whole gate oxide area along *L* will be affected even for a single 2 μA-BD path. The chemical composition at the center of the percolation path changes from $SiO_{1.3}$ to $SiO_{1.0}$ as it evolves from digital to analog BD, which is believed to be responsible for the increment in the gate current leakage when $V_{gstress} > V_{crit}$.

We would like to acknowledge Ministry of Education (MOE) Grant No. T206B1205 and NTU RGM 33/03, and thank Dr. Michel Bosman for technical discussion.

References

[1] V. L. Lo, K. L. Pey, C. H. Tung and X. Li, *Tech. Dig. – Int. Electron Devices Meet*. pp. 497 (2007).

[2] V. L. Lo, K. L. Pey, C. H. Tung and D. S. Ang, *Proc. IEEE 45th Int. Rel. Phys. Symp*. pp. 576 (2007)

[3] C. H. Tung, K. L. Pey, L. J. Tang, M. K. Radhakrishnan, W. H. Lin, F. Palumbo and S. Lombardo, *Appl. Phys. Lett.* **83**, 2223 (2003).

[4] B. Kaczer, *IEEE Trans. Electron Devices* **49**, 507 (2002).

[5] P. E. Batson, *Nature* **366**, 727 (1993).

[6] X. Li, C. H. Tung and K. L. Pey, *Appl. Phys. Lett.* **93**, 072903 (2008).

[7] R. F. Egerton, *Ultramicroscopy* **107**, 575 (2007).

[8] D. A. Muller, T. Sorsch, S. Moccio, F. H. Baumann, K. Evans-Lutterodt and G. Timp, *Nature* **399**, 758 (1999).